Transactions of the Korean Nuclear Society Spring Meeting
Jeju, Korea, May18-19, 2017

Drop Behavior Analysis of Control Rod Assembly for PGSFR using HEXCON code

K. H. Yoon[a*], H.S. Lee[b], J.S. Cheon[b]
a LWR Fuel Technology Development Division, KAERI, 989-111 Daedeok-daero, Yuseong-gu, Daejeon, khyoon@kaeri.re.kr
b Next-generation Fuel Development Division, KAERI, 989-111 Daedeok-daero, Yuseong-gu, Daejeon
** Corresponding author: khyoon@kaeri.re.kr*

1. Introduction

The PGSFR core is a heterogeneous, uranium-10% zirconium (U-10Zr) metal alloy fuel design with 112 assemblies: 52 inner core fuel assemblies, 60 outer core fuel assemblies, 6 primary control assemblies, 3 secondary control assemblies, 90 reflector assemblies, and 174 B_4C shield assemblies and 66 in-vessel storage assemblies. The PGSFR core configuration is shown in Fig. 1. This core is designed to produce 150 MWe with an average temperature rise of 155 ℃. The inlet temperature is 390 ℃ and the bulk outlet temperature is 545 ℃. The active core height is 900 mm and the gas plenum length is 1,250 mm.

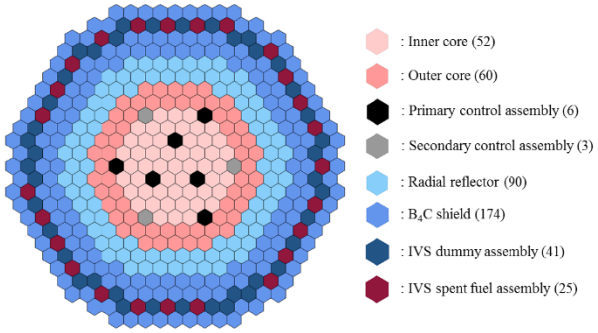

Fig.1 Core plan configuration of 150 MWe for PGSFR.

To evaluate the control rod drop behavior in the core under submerged and coolant flow condition of sodium, drop analysis has to be executed. The control rod assemblies (CRAs) are to be inserted into the reactor core within a stipulated time by scram action before the plant parameters exceed the design safety limits. Of course, the gravity assisted drop of the CRA is opposed by the forces of fluid drag, buoyancy, pressure and shear acting on the control rods (CRs). The simple equation of motion cannot be used to evaluate the drop behavior of the CRA because the CRA is composed of several structural parts. So, hydraulic circuit analysis (HCA) is introduced to predict the drop behavior of the CRA.

2. Drop Analysis

2.1 Overall control assembly

The control assembly (CA) is composed of the control rod assembly, handling socket, hexagonal duct, damper and inlet nozzle. The CRA is composed of the upper/lower adapter, inner hexagonal duct, 19 CRs, clamping/piston head and mounting rails. The CRs are composed of the upper/lower end cap, cladding, plenum spring, wire, Al_2O_3 spacer and B_4C pellet.

The CRA is moved up and down by the gripper of the CRDM. There are two kinds of the CAs in the core. One is the primary CA (PCA), the other is the secondary CA (SCA). The six PCAs are used to control the excess reactivity of the core during operation and to shutdown for emergency condition. The SCAs are used for shutdown core and, for diversity, are separately actuated.

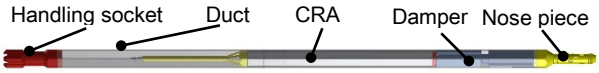

Fig. 2 Schematic drawing of a PCA for PGSFR.

The plan view of the CRA is shown in Fig. 3. There are two flow paths. One is the inner flow path which involves flow inside of the CRA (flow path A), the other is the outer flow path, which is composed of the inner and outer hexagonal ducts (flow path B).

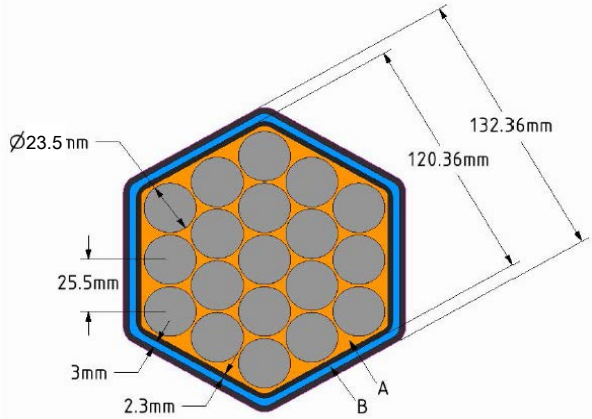

Fig. 3 Plan view of the CRA for PGSFR.

2.2 Hydraulic circuit analysis and Boundary condition

In order to evaluate the drag force of the CRA under submerged and fluid flowing condition, the pressure and flow information at each region are needed. For this, the HCA is introduced to obtain the flow distribution at the inside and outside of the CRA. In this HCA, the local flow paths are replaced the mass balance equation with the piping component, the pressure loss of the fluid, the fluid velocity, and the flow distribution of each piping components is then evaluated. The HCA of the CRA is depicted in Fig. 3.

The initial condition for the drop analysis of the CRA is as follows. The mass flow rate at the inlet is 2.11 kg/s,

the initial drop height is 1.0 m. The time increment is 0.001 second, and the convergence criterion is 10^{-4}.

2.3 Governing equations

The governing equation is constituted of two equations. One is the equation of motion, the other is the mass balance equation for fluid flow.

○ Equation of motion

The equation of motion of the CRA is Eq. (1).

$$m\frac{dV}{dt} = mg - \left[F_{pressure}(t) + F_{shear}(t) + F_{buoyancy}(t)\right]$$
$$F_{pressure} = \sum P_{static} \cdot A_{horizontal} \quad \text{(eq. 1)}$$
$$F_{shear} = \sum \left(\frac{f}{8} \cdot \rho \cdot U^2\right) \cdot A_{vertical}$$
$$F_{buoyancy} = \sum P_{hydraulic} \cdot A_{vertical}$$

where m is the CRA mass, V is the falling velocity, g is the gravitational acceleration, ρ is the fluid density, U is the fluid velocity, $F_{pressure}$ is the pressure drag, F_{shear} is the shear drag acting on the surface of the CRA, and $F_{friction}$ is the friction drag.

○ Mass balance equations for fluid flow

The equations for fluid flow of the hydraulic circuit consist of the flow mass balance and the pressure balance in the hydraulic circuit diagram, which are shown in Fig. 4.

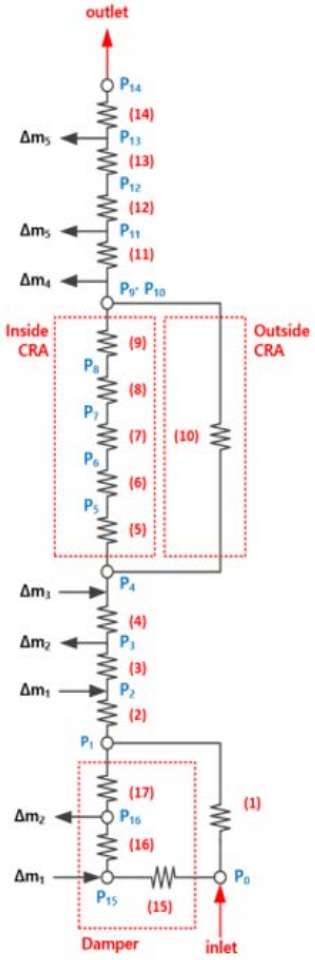

Fig. 4 Hydraulic circuit diagram of the CRA.

$$\boldsymbol{F_1 = m_1 + \Delta m_1 - m_2 - m_3 = 0} \quad \text{(eq. 2)}$$
$$\boldsymbol{F_2 = \Delta P_2 - \Delta P_3 = 0} \quad \text{(eq. 3)}$$

where m_1 is flow rate at the inlet, and m_2 and m_3 are the inside and outside flow rates at the dual hexagonal duct.

○ Flow distribution of the split flow path

The Newton-Raphson iteration method is introduced to evaluate the continuous equation of pressure loss in the inside and outside flow paths of the CRA.

$$\begin{bmatrix} \boldsymbol{m_2^{k+1}} \\ \boldsymbol{m_3^{k+1}} \end{bmatrix} = \begin{bmatrix} \boldsymbol{m_2^{k}} \\ \boldsymbol{m_3^{k}} \end{bmatrix} - [\boldsymbol{J}]^{-1} \begin{bmatrix} \boldsymbol{F_1(m_2^k, m_3^k)} \\ \boldsymbol{F_2(m_2^k, m_3^k)} \end{bmatrix} \quad \text{(eq. 4)}$$

where the superscript is the number of iterations, and [J] is a Jacobian matrix.

The Jacobian matrixes for F_1 and F_2 are as follows.

$$[\boldsymbol{J}] = \begin{bmatrix} \frac{\partial F_1}{\partial m_2} & \frac{\partial F_1}{\partial m_3} \\ \frac{\partial F_2}{\partial m_2} & \frac{\partial F_2}{\partial m_3} \end{bmatrix} \quad \text{(eq. 5)}$$

2.4 Flow chart of the HEXCON code

The flow chart of the HEXCON code is shown in Fig. 5. The variable names and the HEXCON code are summarized in Table 1.

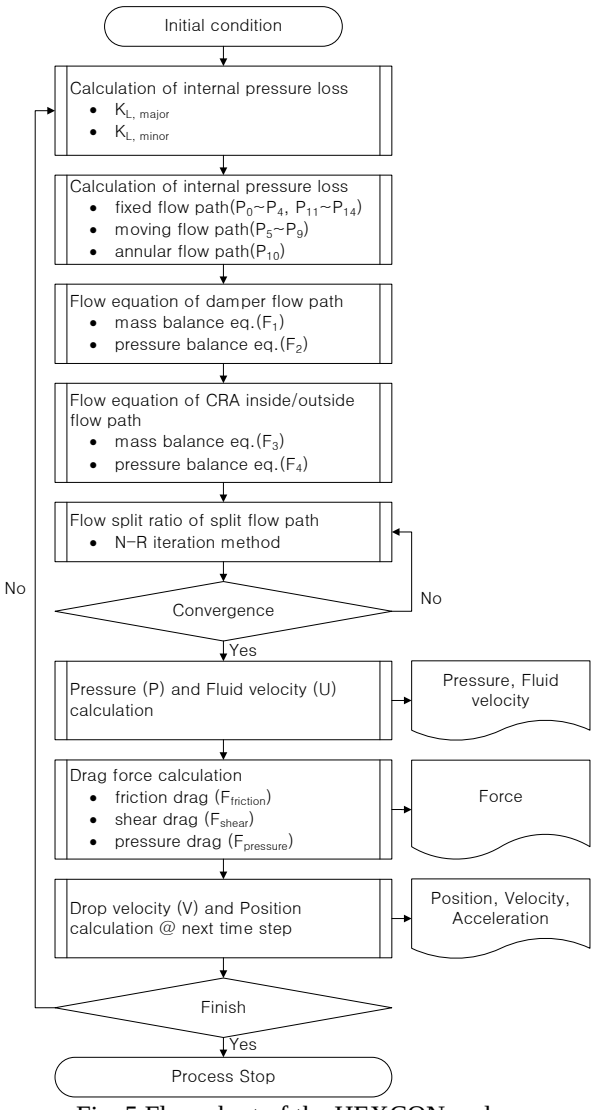

Fig. 5 Flow chart of the HEXCON code.

Table 1. Variable names in the mathematical model and the HEXCON code

Mathe. Model	HEXCON	Mathe. Model	HEXCON
ρ	rho	f_{lam}	f_lam
μ	mu	$f_{transient}$	f_transient
m_{inlet}	m_inlet	$f_{blasius}$	f_blasius
dt	dt	f_1	f1
S	S	K_1	K1
V	V	K_{1_major}	K1_major
α	alpha	K_{1_lam}	K1_lam
β	beta	K_{1_turb}	K1_turb
D_{inlet}	D_inlet	K_{1_turb}	K1_minor
L_{inlet}	L_inlet	$dt\_P1_{friction}$	dt_P1_friction
t_{hex}	t_hex	Ψ	Psi
π	M_PI	k_nonc	k_nonc
A_{pis_rod}	A_pis_rod	$dt\_P1_{spatial}$	dt_P1_spatial
D_{H1}	D_H1	dt_P1	dt_P1
L_1	L1	F_1	F1
A_1	A1	dF_{1_15}	dF1_15
Δm_1	dt_m1	inc_{15}	inc15
Re_1	Re1	F_{p1}	F_p1
U_1	U1	$F_{pressure}$	F_pressure

3. Analysis results

3.1 CRA drop velocity result

The analysis results using HEXCON code are compared with the test results. The analysis conditions for validation are as follows. The tests are executed in the KAERI test facility under room temperature water condition. In these test conditions, the nominal flow rate is 0.46 kg/s. Therefore, the fluid flow conditions are 0, 0.23, 0.46, 0.69, and 0.92 kg/s. Those values correspond to the flow rates of 0, 50, 100, 150 and 200%, respectively.

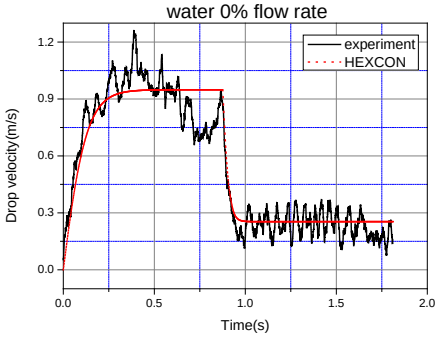

(a) 0% flow rate case

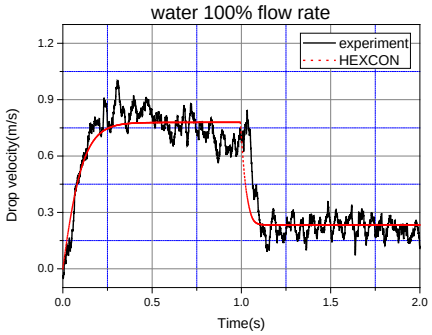

(b) 100% flow rate case

Fig. 6 Comparison result for CRA drop velocity between experiment and analysis.

In this paper, only the representative validation cases are shown in Fig. 6. They are cases of 0 and 0.46 kg/s flow rate taken from the immersed and 100% flow rate cases, respectively. Drop velocity curves of the CRA are compared for the experiment and the HEXCON analysis cases.

In these graphs, the HEXCON analysis results are in good agreement with the experimental results. However, the drop velocity fluctuation is very severe, so it is very difficult to extract the maximum drop velocity. These results are obtained from piecewise linear curve fitting. Deviations between the two methods are summarized in Table 2.

Table 2. Maximum drop velocity deviation between experiment and HEXCON analysis

Flow rate	Max. drop velocity [m/s]		deviation [%]
	experiment	HEXCON	
0 %	0.91	0.95	**4.4**
100 %	0.77	0.78	**1.3**

3.2. CRA position vs. time

Similar to the drop velocity, the CRA position with respect to time is shown in Fig. 7. The deviation between the two methods is approximately 5%. Therefore, it can be concluded that the HEXCON code is useful for the prediction of the drop behavior of the CRA under immersed and fluid flow conditions.

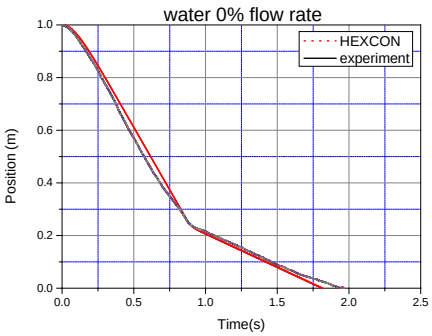

(a) 0% flow case

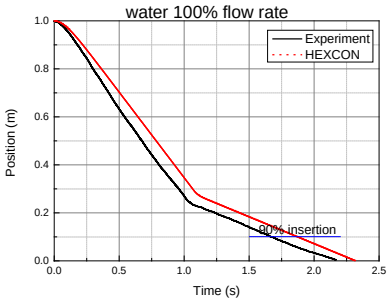

(b) 100% flow case

Fig. 7 Comparison results for CRA position vs. time between test and analysis.

Table 3. CRA complete drop time deviation between experiment and HEXCON analysis

Flow rate	Drop time [s]		deviation [%]
	experiment	HEXCON	
0 %	1.9	1.8	**-5.3**
100 %	2.2	2.3	**4.5**

3.3 CRA design modification

Based on the validation results, the revised CRA design is carried out using the HEXCON code. The PGSFR design criteria for CRA insertion is as follows. From a safety analysis viewpoint, the complete insertion time of the CRA is 2.0 seconds under 100% sodium flow condition. Up to 90% insertion, the CRA is dropped with the maximum drop velocity, then the drop velocity decelerates incorporating viscous damping between the piston head and the flow hole of the damper. The diametral clearance in the dashpot region is 0.5 mm. The reducing rate of the drop velocity is approximately 67% due to viscous damping, there is no necessity to separate the hydraulic shock absorber device in the core. The terminal drop velocity of 0.3 m/s will not affect the structural soundness of the reactor internals.

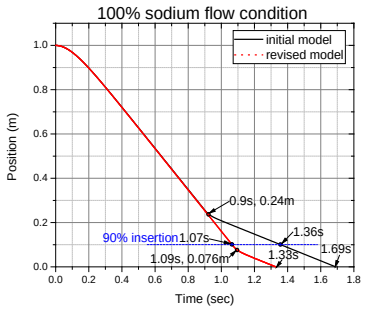

(a) CRA position vs. time

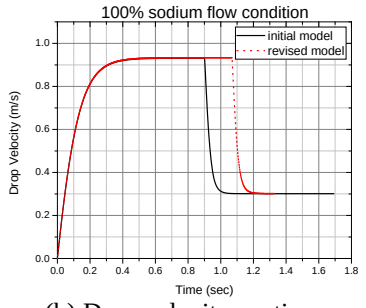

(b) Drop velocity vs. time

Fig. 8 Drop behavior of the CRA for PGSFR.

For a length of the lower adapter rod of 125 mm, the 90% insertion time is 1.07 second, the complete insertion time is 1.33 seconds. Therefore, the final drop time including the delay time of 0.38 seconds is 1.71 seconds, which is shown in Fig. 8. This is less than 2.0 seconds, and so the design target for the drop time is satisfied. The delayed time is the average value from the many times experimental results.

The final design parameters of the CRA for PGSFR are summarized in Table 4.

Table 4. Design parameters of CRA for PGSFR

Parameters	value
CR outside diameter	23.5 mm
CR pitch	25.5 mm
Wire outside diameter	1.9 mm
# of control rod	19
CRA mass	57 kg
Diametral gap @inner/outer hexagonal duct	3.0 mm
Diametral gap @piston head/flow hole of damper	0.5 mm
Mass flow rate for CA	2.11 kg/s

4. Conclusion

Mathematical modeling of the CRA under immersed and the fluid flow conditions is carried out. The developed numerical analysis results are compared with the experimental results and validated. The CRA design for PGSFR is satisfied with the stipulated design criteria. In addition to this, the sophisticated damper sufficiently decelerate the drop velocity of the CRA. Therefore, it is demonstrated that this system has no negative impact on the structural soundness of the reactor internals.

ACKNOWLEDGEMENTS

This project has been carried out under the nuclear R&D program by MISP (Ministry of Science, ICT and Future Planning in Republic of Korea).

REFERENCES

[1] KAERI Document, 2016, Primary Control Rod Assembly, No. SFR-175-FP-101-001, Rev.01.

[2] KAERI Document, 2016, Control Rod Assembly Mechanical Design Data, No. SFR-175-FP-490-001, Rev.01.

[3] KAERI Document, 2015, Drop Performance Test Report of Control Rod Assembly, SFR-730-DM-458-002.

[4] Rajan Babu, V., Thanigaiyarasu G. and Chellapandi, P., 2014, “Mathematical modelling of performance of safety rod and its drive mechanism in sodium cooled fast reactor during scram action,” Nuclear Engineering and Design, Vol. 278, pp.601-607.

[5] Cengel, Y.A., Cimbala, J.M., 2006, Fluid Mechanics: Fundamentals and Applications, New York, McGraw-Hill.

[6] Young, D.F., Munson, B.R. and Okiishi, T.H., 2004, A Brief Introduction to Fluid Mechanics 3rd Edition, New Jersey, United states, John & Wiley.

[7] Idelchik, I. E., 2007, Handbook of Hydraulic Resistance, 4th Edition Revised and Augmented, CT, United states, Begell House Publishing.